Electrocatalytic properties of La$_{1-x}$Cu$_x$CoO$_3$ (0 ≤ x ≤ 0.8) film electrodes for oxygen evolution in alkaline medium: Part II. A comparative study

Manish Kumar Yadav[a], Basant Lal[b] & Narendra Kumar Singh[a],*

[a]Department of Chemistry, Faculty of Science, University of Lucknow, Lucknow 226 007, India

[b]Department of Chemistry, Institute of Applied Science and Humanities, G.L.A. University, Mathura 281 406, India

Email: nksbhu@yahoo.com/ singh_narendra@lkouniv.ac.in

The present study is concerned with the preparation of perovskite-type oxide film electrodes of La, Cu and Co having composition La$_{1-x}$Cu$_x$CoO$_3$ (0 ≤ X ≤ 0.8) on Ni conducting support and study of their electrocatalytic properties towards oxygen evolution reaction (OER) in alkaline medium. Materials have been synthesized by using malic acid sol-gel route at pH 4.00. X-ray diffraction study of the material indicated the formation of almost pure perovskite phase with hexagonal crystal geometry. The electrocatalytic activity of the material has been determined in three electrode single compartment glass cell. Techniques used in the electrochemical studies are cyclic voltammetry (CV), oxide roughness factor and anodic polarization (Tafel plot). Each cyclic voltammogram exhibits an anodic and a corresponding cathodic peak prior to the oxygen evolution reaction. The observed anodic and cathodic peak potential values are 553±31 and 312±27 mV, respectively. The study of anodic polarization curve indicates that the oxide with 0.6 mol Cu-substitution (j_a = 182.4 mA cm^{-2} at 750 mV) shows highest electrocatalytic activity with lowest Tafel slope value (b = 65 mV decade^{-1}) towards OER. Thermodynamic properties of the material have also been investigated by recording the anodic polarization curve at different temperatures. The value of electrochemical activation energy has been found to be lowest with most active 0.6 mol Cu-substituted oxide material. Electrocatalytic activities of the oxide electrodes, so obtained, have been compared with the similar oxide prepared at 3.75 pH.

Keywords: Sol-gel route, Perovskite-type oxide, Powder X-ray diffraction (XRD), Electrocatalytic activity, Thermodynamic parameters, Roughness factor

Perovskite-type oxides with general formula ABO$_3$, where A is lanthanides (mainly La) and B is transition metals (like Ni, Co or Mn) are well known versatile materials with applications to efficient electrocatalysts[1-11] for water electrolysis and solid oxide fuel cells[12-14]. In the early stage of investigation, these materials were mainly prepared at higher temperature[15-19] using conventional ceramic and thermal decomposition methods. These methods produced materials of large particle size with low specific surface area. During the past few decades, some low temperature synthetic routes[20-23] using solid organic precursors like malic acid, citric acid, polyacrylic acid etc., have been reported to produce oxides with high specific surface area. By adopting these methods, Singh *et al.,*[24-35] prepared LaCoO$_3$, LaMnO$_3$, LaNiO$_3$ with their Sr, Pb-substituted derivatives and studied their electrocatalytic properties for OER in alkaline medium. They observed that these materials showed much better electrocatalytic activity than those previously prepared by conventional ceramic and thermal decomposition methods.

Recently, Lal *et al.,*[36] prepared La$_{1-x}$Sr$_x$CoO$_3$ (0 ≤ x ≤ 0.4) by stearic acid sol-gel method and studied their physicochemical (IR, XRD, SEM) and electrochemical (impedance, steady-state anodic polarization) properties for OER. The oxide roughness factor and the apparent electrocatalytic activity of the Sr-substituted lanthanum cobaltates were more or less similar to Sr-substituted lanthanum manganite prepared by malic acid and polyacrylic acid sol-gel route. Recently[37], by adopting citric acid-ethylene glycol precursor route, we reported the electrocatalytic properties of Sr-substituted lanthanum cobaltate towards OER in alkaline medium.

It is also well known that the interfacial properties as well as electrocatalytic properties of these materials are strongly influenced by preparation variables, such as, concentration and pH of the starting solution,

temperature, methodology, nature of the starting material used and metal ion substitution. In view of the above, we studied the electrocatalytic properties of Cu-substituted lanthanum cobaltate[38] obtained at pH = 3.75 by using malic acid sol-gel route[20,32] and found good results towards OER. In the synthesis of oxide material, pH of the starting solution has a vital role to improve the physicochemical property of the material. The solubility and homogeneity of the metal salts can be improved by increasing the pH of the starting solution close to 7.00. By considering these facts, we extended our work and prepared similar perovskite oxides at pH = 4.00 and studied their electrocatalytic properties with regards to OER. In the present paper, we reported the comparative results of the electrocatalytic behaviour of the oxide electrode obtained at both pH.

Experimental

Perovskite-type oxides lanthanum cobaltate with composition $La_{1-x}Cu_xCoO_3$ (x = 0.0, 0.2, 0.4, 0.6 and 0.8) were synthesized by using the method described elsewhere[20,32]. Purified chemicals and reagents purchased from Merck and Qualigens were used in every preparation. In this, excess quantity of malic acid was added to 500 mL aqueous solution of nitrates of La, Cu and Co dissolved in stoichiometric ratio. The pH of this solution was maintained to 4.00 by adding ammonia solution (28%) dropwise. The solution was then kept on a water bath to evaporate the solvent. After certain time, the sol was converted into gel, which decomposed to yield powder at higher temperature. In order to get the desired material, the powder was crushed in agate pestle and mortar followed by heat treatment at 650 °C for 5 h in a PID controlled electrical furnace (ASCO, India).

Perovskite phase of the material was confirmed by recording X-ray diffraction (XRD) pattern. For the purpose, the equipment PANalytical XPERT-PRO Diffractometer (Model PW3050/60) having Radiation Source: Cu-K$_\alpha$ and wave length (λ): 1.54048 Å was used. The morphology of the material was examined in the form of film on Ni-support by using scanning electron microscope (JOEL JSM 6490LV). The electrochemical characterization has been performed in the form of oxide film electrode on Ni-support. The oxide film was prepared by painting the slurry of oxide with Triton X-100 as described in the literature[25]. The treatment of Ni-support and electrical connection with the oxide film were done in a similar way as described earlier[25,30].

The electrochemical characterization of the oxide electrodes was performed in three electrode single compartment glass cell. In the cell arrangement, counter and reference electrodes were platinum foil (~2 cm^2) and Hg/HgO/1M KOH (E° = 0.098 V vs NHE at 25 °C), respectively. The working electrode was the oxide film electrode. Techniques used in the study were cyclic voltammetry (CV), roughness factor and anodic polarization curve (Tafel plot). An electrochemical work station (Gamry Reference 600 ZRA) equipped with potentiostat/ galvanostat and corrosion and physical electrochemistry software was used to run the experiments. Experimental data were recorded on the desktop computer (HP). In order to minimize the solution resistance (iR drop), a Luggin capillary (agar-agar and potassium chloride gel) was employed between working and reference electrode. The relation, $\eta = E - E_{O_2/OH^-}$, was used to estimate overpotential (η) values, where E and E_{O_2/OH^-} (= 0.303 V vs. Hg/HgO) are the applied potential[39] across the catalyst/ 1 M KOH interface and the theoretical equilibrium Nernst potential in 1 M KOH at 25 °C, respectively.

Results and Discussion

Surface Morphology

Scanning electron micrograph (SEM) of oxides was taken in the form of film on Ni support and shown in Fig. 1(a–e). Morphology of each oxide film was observed to be similar in nature. Materials are distributed homogeneously with some porous appearance. The pH of the starting solution strongly affected the morphology of the material. The texture of the similar oxides prepared[38] at pH = 3.75 was found to be closely packed and compact with some small cracks.

X-ray Diffraction (XRD)

The X-ray diffraction (XRD) pattern of the oxide powder recorded in the 2θ range from 20° to 80° is shown in Fig. 2. As assumed, the XRD patterns of the oxide prepared at pH 3.75 and 4.00 were observed to be similar and have hexagonal geometry. The observed 2θ and their corresponding 'd' values were well matched with JCPDS ASTM file 25-1060. The crystallite size, as calculated by using Scherer's formula[40], was also observed to be almost similar at both pH. This might be due to the very proximity in the pH value. Values of crystallite size were ranged between 24–38 nm.
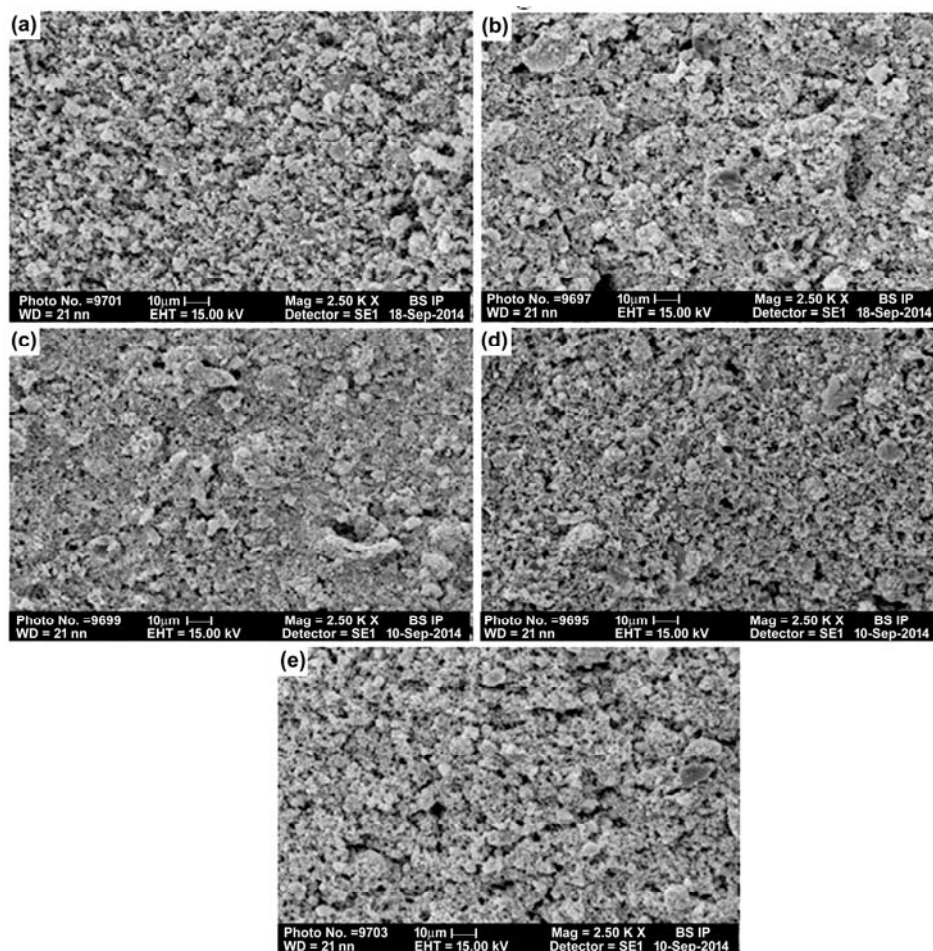
Fig. 1 — SE Micrographs of oxide film on Ni sintered at 650 °C for 5 h. a) LaCoO$_3$, b) La$_{0.8}$Cu$_{0.2}$CoO$_3$, c) La$_{0.6}$Cu$_{0.4}$CoO$_3$, and, d) La$_{0.4}$Cu$_{0.6}$CoO$_3$, and e) La$_{0.2}$Cu$_{0.8}$CoO$_3$.
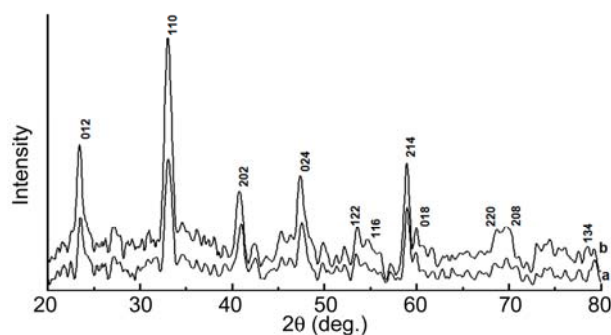

Fig. 2 — X-ray diffraction patterns of La$_{1-x}$Cu$_x$CoO$_3$, sintered at 650 °C for 5 h; (a) x = 0 mol and (b) x = 0.4 mol.

Cyclic Voltammetry (CV)

The cyclic voltammetric (CV) curve of each oxide film electrode on Ni was recorded in the potential region 0.0 to 0.7 V at a scan rate 20 mV sec^{-1} in 1 M KOH solution at 25 °C. The CV curve of the oxides were obtained at pH 4.00 is shown in Fig. 3. Each voltammogram exhibited a pair of redox peaks, one
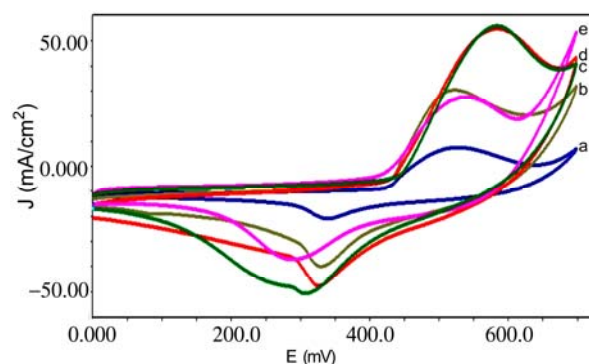

Fig. 3 — Cyclic voltammograms of pure and Cu-substituted film electrode on Ni at scan rate of 20 mV sec^{-1} in 1M KOH (25 °C); a) LaCoO$_3$, b) La$_{0.8}$Cu$_{0.2}$CoO$_3$, c) La$_{0.2}$Cu$_{0.8}$CoO$_3$, d) La$_{0.6}$Cu$_{0.4}$CoO$_3$, and, e) La$_{0.4}$Cu$_{0.6}$CoO$_3$.

anodic (553±31 mV) and a corresponding cathodic (313±27 mV) peak prior to the oxygen evolution reaction. Similar nature of the CV curve was also observed with the oxides[38] prepared at pH 3.75.

The peak separation potential and formal redox potential calculated from the CV curves were found to be 233±45 and 434±22 mV, respectively. The results, so obtained, are shown in Table 1. The data given in the table showed that the pH variation in the preparation of oxides has almost negligible influence on the cyclic voltammetric parameters.

The effect of variation of scan rate (20–120 mV sec^{-1}) on cyclic voltammograms was also studied with each oxide electrode. A representative CV curve at different scan rates for $Ni/La_{0.4}Cu_{0.6}CoO_3$ is shown in Supplementary Data, Fig. S1. The feature of CV curves, so obtained, was found to be similar to that observed at the scan rate of 20 mV sec^{-1}. The estimated values of cyclic voltammetric parameters as given in Table 2 at different scan rates indicate that both anodic and cathodic peaks shift to either direction with the 6-fold increase in the scan rate. The shifting of potential in the cathodic side is relatively less as compared to that found in anodic side. The observed shifts in the peak potential were 100–143 mV and 41–88 mV in anodic and cathodic side, respectively. Further, it is found that both anodic and cathodic peak current values increased linearly

with increase in the scan rates. The ratio of anodic and cathodic peak current is greater than unity. This indicates that redox process is irreversible.

The voltammetric charge as determined by integrating both anodic and cathodic sides of CV curve up to the potential just prior to the OER was observed to decrease as the scan rate is increased from 20 to 120 mV sec^{-1}. The voltammetric charge (q) is plotted against (scan rate)$^{-1/2}$ for each oxide electrocatalyst and shown in Supplementary Data, Fig. S2. The nature of the plot is similar to that obtained in the case of oxide electrode prepared at pH = 3.75. The observed straight line indicated the diffusion-controlled process of the surface redox couple under given potential conditions.

Roughness factor

Electrochemically active area of the oxide electrode was determined in terms of roughness factor. For the purpose, cyclic voltammograms were recorded in a small potential region (0.0–0.1 V) at varying potential scan rates in 1M KOH at 25 °C. A representative voltammogram is shown in the Supplementary Data, Fig. S3. Charging current density (j_{cap}) at each scan rate was measured at the middle (E = 50 mV) of potential scanned. A plot of charging current density (j_{cap}) vs scan rate for each oxide electrodes was constructed and shown in Supplementary Data, Fig. S4. Double layer capacitance (C_{dl}) was estimated by measuring the slope of straight line. The relative roughness factor was calculated by using relation[41] $R_F = C_{dl}/60$ and values obtained, are given in the Table 3. In each case, 60 μF cm^{-2} was assumed as the C_{dl} for ideally smooth oxide surface. It is clear that no regular trend is observed in the active surface area of the oxide electrodes prepared at both pH values as observed from Table 3.

Electrocatalytic activity

The electrocatalytic activity for OER of oxide film electrodes on Ni was determined by recording the anodic polarization curves at scan rate of 0.2 mV sec^{-1} in 1 M KOH at 25 °C. The polarization curve, thus obtained, is shown in Fig. 4. Each polarization curve shows similar nature regardless the introduction of Cu for La in the base oxide ($LaCoO_3$). Values of the Tafel slope (b) and electrocatalytic activity in terms of current density as well as overpotential were estimated from the polarization curve and given in Table 3. Values of Tafel slope of the oxide electrode prepared at

Table 1 — Values of the cyclic voltammetry parameters of Ni/$La_{1-x}Cu_xCoO_3$($0 \leq X \leq 0.8$) in 1M KOH at 25 °C (scan rate = 20 mVsec^{-1})

Electrode	E_{Pa}/ mV	E_{Pc}/ mV	ΔE_p/ mV	$E°= (E_{Pa}+E_{Pc})/2$/ mV
$LaCoO_3$	527	339	188	433
	(532)	(322)	(210)	(427)
$La_{0.8}Cu_{0.2}CoO_3$	522	330	192	426
	(523)	(296)	(227)	(409)
$La_{0.6}Cu_{0.4}CoO_3$	584	326	258	455
	(610)	(294)	(316)	(452)
$La_{0.4}Cu_{0.6}CoO_3$	538	286	252	412
	(523)	(321)	(202)	(422)
$La_{0.2}Cu_{0.8}CoO_3$	584	306	278	445
	(553)	(289)	(264)	(421)

Values given in parentheses corresponds to the similar oxides[38] obtained at pH = 3.75

Table 2 — Cyclic voltammetric parameters for the Ni/$La_{0.4}Cu_{0.6}CoO_3$ at different scan rates in 1 M KOH at 25 °C

Scan rate/ mVsec^{-1}	E_{Pa}/ mV	E_{Pc}/ mV	$\Delta E = E_{Pa} - E_{Pc}$/ mV	$E° = (E_{Pa} + E_{Pc})/2$/ mV	$\|j_{Pa}\|$/ mA cm^{-2}	$\|j_{Pc}\|$/ mA cm^{-2}	$\|j_{Pa}\|/\|j_{Pc}\|$	q/ mC cm^{-2}
20	538	286	252	412	37.7	26.9	1.4	666.0
40	597	260	337	429	58.8	40.6	1.4	592.7
60	634	236	398	435	75.1	50.6	1.5	521.3
80	650	225	425	431	89.8	58.7	1.5	458.1
100	665	211	454	438	102.0	65.6	1.6	409.0
120	675	198	477	437	113.3	71.4	1.6	370.0

Table 3 — Electrode kinetic parameters for oxygen evolution reaction on La$_{1-x}$Cu$_x$CoO$_3$ (0 ≤ x ≤ 0.8) electrodes in 1 M KOH at 25 °C

Electrode	Tafel slope / mVd^{-1}	Roughness Factor (R$_F$)	Order (p)	E/ mV at j$_a$ (mA cm^{-2})		j/ (mA cm^{-2}) at E = 750 mV	
				100	300	j$_a$	j$_t$×10^2
LaCoO$_3$	80	803	~1	727	822	138.1	17.2
	(78)	(176)	(~1)	(874)	(1204)	(39.9)	(22.7)
La$_{0.8}$Cu$_{0.2}$CoO$_3$	76	1227	~1	779	916	66.3	5.4
	(80)	(1244)	(~1)	(844)	(1142)	(49.2)	(3.9)
La$_{0.6}$Cu$_{0.4}$CoO$_3$	75	1435	~1	773	906	79.1	5.5
	(90)	(291)	(~1)	(734)	(951)	(111.6)	(38.4)
La$_{0.4}$Cu$_{0.6}$CoO$_3$	65	253	~1	711	791	182.4	72.1
	(88)	(818)	(~1)	(822)	(1083)	(59.3)	(7.2)
La$_{0.2}$Cu$_{0.8}$CoO$_3$	75	1796	~1	741	853	111.4	6.2
	(90)	(671)	(~1)	(782)	(1018)	(70.2)	(10.5)

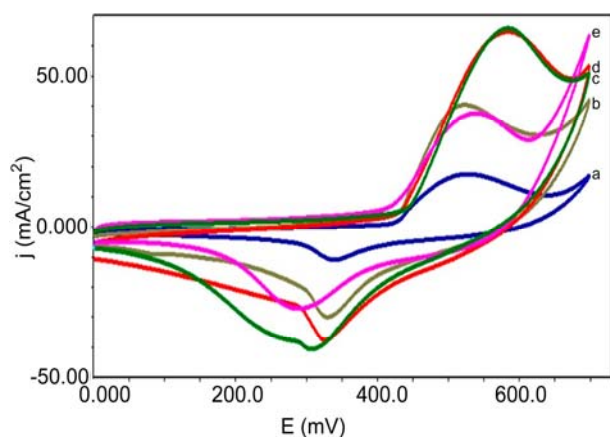Values given in parentheses corresponds to the similar oxides[38] obtained at pH = 3.75.

Fig. 4 — Tafel plots for the pure and Cu-substituted LaCoO$_3$ films on Ni in 1M KOH (25 °C); scan rate: 0.2 mVsec^{-1}; a) La$_{0.8}$Cu$_{0.2}$CoO$_3$, b) La$_{0.6}$Cu$_{0.4}$CoO$_3$, c) La$_{0.2}$Cu$_{0.8}$CoO$_3$, d) LaCoO$_3$, and, e) La$_{0.4}$Cu$_{0.6}$CoO$_3$.

pH 4.00 (65–80 mV decade^{-1}) was found to be lower as compared to those prepared at pH 3.75 (78–90 mV decade^{-1}). The decrease in the Tafel slope at pH 4.00 might be due the slight improvement in the texture of the material. However, no regular trend was observed in the case of electrocatalytic activity of the materials. In terms of apparent current density (j$_a$) at 750 mV, except La$_{0.6}$Cu$_{0.4}$CoO$_3$, all other oxides prepared at pH 4.00 showed higher electrocatalytic activity than those prepared at pH 3.75. However, in terms of true current density (j$_t$), which is calculated by dividing the apparent current with roughness factor, the oxide, La$_{0.6}$Cu$_{0.4}$CoO$_3$ (j$_t$ = 38.4×10^{-2}) prepared at pH 3.75 has highest electrocatalytic activity. At E = 750 mV, the following electrocatalytic activity order has been observed in the oxide electrode obtained at pH 4.00:
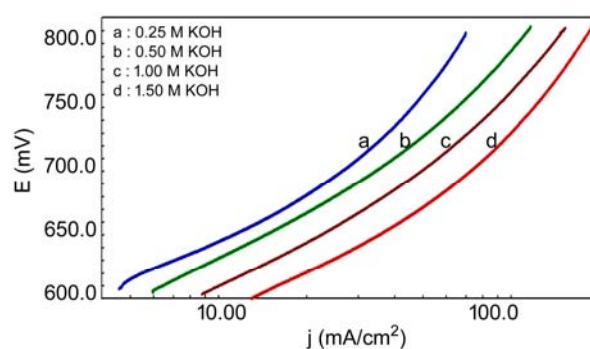

Fig. 5 — Tafel plots for oxygen evolution on the La$_{0.4}$Cu$_{0.6}$CoO$_3$ film on Ni at varying KOH concentrations (μ = 1.5) at 25 °C.

La$_{0.4}$Cu$_{0.6}$CoO$_3$ (j$_a$ = 182.4 mA cm^{-2}) > LaCoO$_3$ (j$_a$ = 138.1 mA cm^{-2}) > La$_{0.2}$Cu$_{0.8}$CoO$_3$ (j$_a$ = 111.4 mA cm^{-2}) > La$_{0.6}$Cu$_{0.4}$CoO$_3$ (j$_a$ = 79.1 mA cm^{-2}) > La$_{0.8}$Cu$_{0.2}$CoO$_3$ (j$_a$ = 66.3 mA cm^{-2}).

The OER study has been carried out with each oxide electrode in varying KOH concentration (Fig. 5) for the determination of order of reaction. The ionic strength of each KOH solution was maintained constant (μ = 1.5) by using KNO$_3$ as an inert electrolyte. From the data of the polarization curve, a plot of log j vs log [OH$^-$] (Fig. 6) was constructed at a constant applied potential (E = 650 mV). The order of reaction was estimated by measuring the slope of the straight line and found to be unity with each oxide electrode (Table 3). Values of Tafel slope and reaction order reveals that oxides prepared at both pH have almost similar mechanistic path towards OER.

Thermodynamic parameters for OER have also been investigated with each oxide electrode. For the purpose, anodic polarization curve (Fig. 7) was recorded in 1 M KOH at different temperatures. The Arrhenius plot of log j vs 1/T, as shown in Fig. 8, was constructed at a
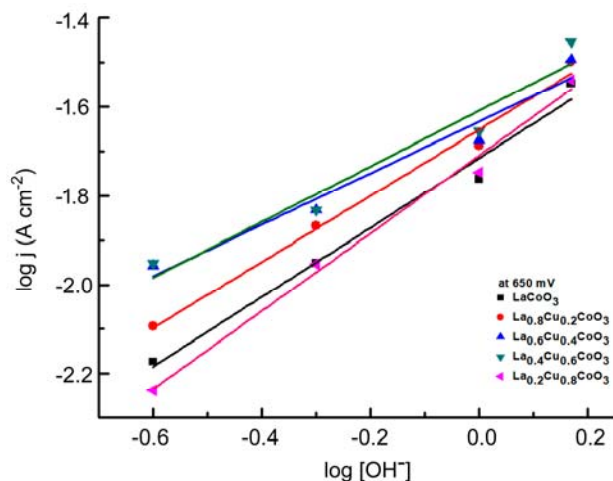
Fig. 6 — Plot of log j vs log [OH⁻] at a different applied potential for $La_{0.6}Cu_{0.4}CoO_3$ films on Ni at 25 °C.

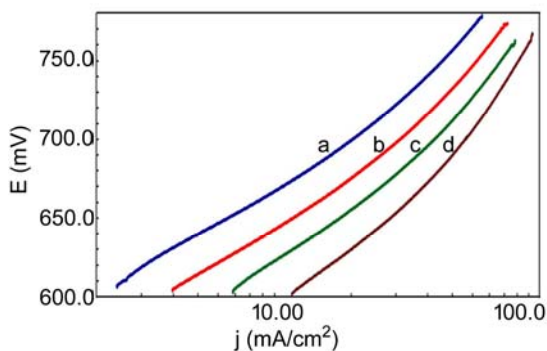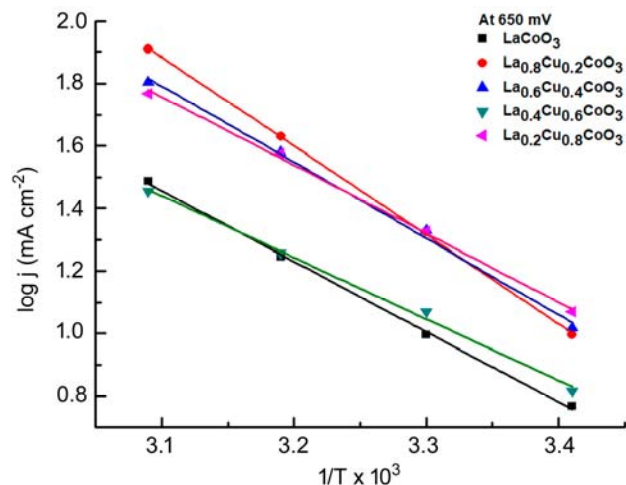Fig. 8 — The Arrhenius plot at a constant applied potential (650 mV) for $La_{1-x}Cu_xCoO_3$ ($0 \leq x \leq 0.8$) in 1 M KOH.

Fig. 7 — Tafel plots for oxygen evolution on the $La_{0.4}Cu_{0.6}CoO_3$ film on Ni at different temperatures in 1 M KOH; a) 20 °C, b) 30 °C, c) 40 °C, and, d) 50 °C

Table 4 — Thermodynamic parameters for O_2 evolution on Ni /$La_{1-x}Cu_xCoO_3$ ($0 \leq x \leq 0.8$) in 1 M KOH at 650 mV

Electrode	$\Delta H_{el}^{\circ\#}$ (kJ mol^{-1}) at E = 675 mV	- $\Delta S^{\circ\neq}$ (J deg^{-1} mol^{-1})	α	$\Delta H^{\circ\neq}$ (kJ mol^{-1})
$LaCoO_3$	43.1	174.4	0.7	67.7
	(43.0)	(184.9)	(0.7)	(68.3)
$La_{0.8}Cu_{0.2}CoO_3$	54.4	144.8	0.7	80.2
	(45.3)	(174.1)	(0.7)	(70.0)
$La_{0.6}Cu_{0.4}CoO_3$	46.6	167.6	0.7	72.9
	(35.1)	(195.7)	(0.5)	(52.3)
$La_{0.4}Cu_{0.6}CoO_3$	37.6	189.8	0.9	67.9
	(42.3)	(181.2)	(0.6)	(64.7)
$La_{0.2}Cu_{0.8}CoO_3$	41.8	181.3	0.7	68.0
	(40.2)	(182.7)	(0.5)	(58.3)

Values given in parentheses corresponds to the similar oxides[38] obtained at pH = 3.75

constant applied potential (E = 650 mV). The activation energy was calculated by measuring the slope of the straight line. Other parameters, such as transfer coefficient (α), standard electrochemical energy of activation ($\Delta H_{el}^{\circ\neq}$), standard enthalpy of activation ($\Delta H^{\circ\neq}$) and standard entropy of activation ($\Delta S^{\circ\neq}$) were calculated by using Eqns 1 and 2[42,43]:

$$\Delta H_{el}^{\circ\neq} = \Delta H^{\circ\neq} - \alpha F \eta \qquad \ldots (1)$$

Where, α is the transfer coefficient equal to 2.303RT/bF. The Tafel slope (b) is calculated from the polarization curves obtained at different temperatures. and R, F and T are the gas constant, Faraday constant and absolute temperature, respectively. η is the overpotential.

$$\Delta S^{\circ\neq} = 2.3R \left[\log j + \frac{\Delta H_{el}^{\circ\neq}}{2.3RT} - \log \left(n\omega F \omega C_{OH^-} \right) \right] \ldots (2)$$

Where, ω (= $k_B T/h$) is the frequency term and $n = 2$, k_B and h are the Boltzmann constant and Plank's constant, respectively.

The estimated values of transfer coefficient (α), standard apparent enthalpy of activation, standard enthalpy of activation and entropy of activation are given in Table 4. The table shows that the value of electrochemical activation energy did not follow a regular trend with the oxide electrodes. However, the value was found to be minimum with highly active $La_{0.6}Cu_{0.4}CoO_3$ (35.1 kJ mol^{-1} obtained at pH 3.75) and $La_{0.4}Cu_{0.6}CoO_3$ (37.6 kJ mol^{-1} obtained at pH 4.00) electrodes. Also, it is observed that the value of activation energy decreases with the increase of applied potential and it is well satisfied by the Eqn 1. The highly negative value of $\Delta S^{\circ\neq}$ indicates the presence of adsorption phenomenon in the electrochemical formation of oxygen.

Conclusions

The study indicates that the pH value at the time of preparation strongly affects the morphology of the material. Texture of the oxide film obtained at pH = 4.00 are porous and homogeneously distributed. However, it was found to be closely packed and compact at pH = 3.75. Substitution of Cu for La did not show any regular trend in the electrocatalytic activity. But, 0.6 mol Cu showed highest activity ($j_t = 72.1 \times 10^{-2}$ at E = 750 mV) with lowest activation energy (37.6 kJ mol^{-1}) among the oxides prepared. Tafel slope values were found to be lower with oxides prepared at pH = 4.00.

Supplementary Data

Other supplementary data and cif files associated with this article are available in the electronic form at http://www.niscair.res.in/jinfo/ijca/IJCA_58A(12) 1295-1301_SupplData.pdf.

Acknowledgement

References

1 Trasatti S, *The Electrochemistry of Novel Materials*, edited by Lipkowaski J & Ross P N (VCH Weinheim) 1994, p 207.
2 O'Sullivan E J M & Calvo E J, *Electrode kinetic reaction*, edited by Compton R G (Elsecier, Amsterdam), 1987.
3 Trasatti S, Lodhi G, *Electrodes of conductive metallic oxides, Part B*, edited by Trasatti S (Elsevier, Amsterdam), 1981.
4 Tejuca L G, Feierro J L F & Tascon J M, *Advances in catalysis*, (Academic Press, New York), 36 1991.
5 Ladovos A K & Pomonis P, *J Chem Soc Faraday Trans*, 87 (1991) 3291.
6 Yamazoe N & Teraoka V, *Catal Today*, 8 (1990) 175.
7 Tagawa T & Imai H, *J Chem Soc Faraday Trans*, 84 (1988) 923.
8 Marti P E & Baiker A, *Catal Lett*, 26 (1994) 71.
9 Islam M S, Cherry M & Winch L J, *J Chem Soc Faraday Trans*, 92 (1996) 479.
10 Wendt H & Imarisio G, *J Appl Electrochem*, 18 (1988) 1.
11 Wendt H & Hofmann H, *J Appl Electrochem*, 19 (1989) 605.
12 Minh N Q, *J Am Ceram Soc*, 76 (1993) 563.
13 Anderson H U, *Solid State Ionics*, 52 (1992) 33.
14 Ishigaki T, Yamauchi S, Kishio K, Mizusaki J & Fueki K, *J Solid State Chem*, 73 (1988) 179.
15 Bockris J O M & Otagawa T, *J Electrochem Soc*, 131(2) (1984) 290.
16 Balej J, *Int J Hydrogen Energy*, 10 (1985) 89.
17 Matsumoto Y, Manabe H & Sato E, *J Electrochem Soc*, 127(4) (1980) 811.
18 Wendt H & Plzak V, *Electrochimica Acta*, 28 (1983) 27.
19 Fiori G & Mari C M, *Int J Hydrogen Energy*, 7 (1982) 489.
20 Teraoka Y, Kakebayashi H, Moriguchi I & Kagawa S, *Chem Lett*, 20 (1991) 673.
21 Vidyasagar K, Gopalkrishanan J & Rao C N R, *J Solid State Chem*, 58(1985) 29.
22 Taguchi H, Matsuda D, Nagao M, Tanihata K & Miyamoto Y, *J Am Ceram Soc*, 75 (1992) 201.
23 Skaribas S P, Pomonis P J & Sdoukos A T, *J Mater Chem*, 1 (1991) 781.
24 Vassiliou J K, Hornbostel M, Ziebarth R & Disalvo F J, *J Solid State Chem*, 81 (1989) 208.
25 Tiwari S K, Chartier P & Singh R N, *J Electrochem Soc*, 142(1) (1995) 148.
26 Jain A N, Tiwari S K, Singh R N & Chartier P, *J Chem Soc Faraday Trans*, 91 (1995) 1871.
27 Singh R N, Jain A N, Tiwari S K, Poillerat G & Chartier P, *J Appl Electrochem*, 25 (1995) 1133.
28 Singh R N, Tiwari S K, Singh S P, Jain A N & Singh N K, *Int J Hydr Ener*, 22 (1997) 557.
29 Tiwari S K, Koenig J F, Poillerat G, Chartier P & Singh R N, *J Appl Electrochem*, 28 (1998) 114.
30 Singh R N, Tiwari S K, Singh S P, Singh N K, Poillerat G & Chartier P, *J Chem Soc Faraday Trans*, 92(14) (1996) 2593.
31 Jain A N, Tiwari S K & Singh R N, *Ind J Chem*, 37A (1998) 125.
32 Singh N K, Tiwari S K & Singh R N, *Int J Hydr Ener*, 23 (1998)775.
33 Sharma T, Singh N K, Tiwari S K & Singh R N, *Ind J Engg Mat Sci*, 5 (1998) 38.
34 Singh N K, Lal B & Singh R N, *Int J Hydr Ener*, 27 (2002) 885.
35 Singh R N, Tiwari S K, Sharma T, Chartier P & Koenig J F, *J New Mat Electrochem Syst*, 2 (1999) 65.
36 Lal B, Raghunanda M K, Gupta M & Singh R N, *Int J Hydro Ener*, 30 (2005) 723.
37 Yadav M K, Yadav R, Sharma P & Singh N K, *Int J Electrochem Sci*, 11 (2016) 8633.
38 Singh N K, Yadav M K & Fernandez C, *Int J Electrochem Sci*, 12 (2017) 7128.
39 Singh R N, Pandey J P, Singh N K, Lal B, Chartier P & Koenig J F, *Electrochim Acta*, 45 (2000) 1911.
40 Fradette N, Marsan B, *J Electrochem Soc*, 145(7) (1998) 2320.
41 Marsan B, Fradette N & Beaudoin G, *J Electrochem Soc*, 139(7) (1992) 1889.
42 Singh R N, Singh N K & Singh J P, *Electrochimica Acta*, 47 (2002) 3873.
43 Gileadi E, *Electrode Kinetics* (VCH Publishers Inc New York) 1993, p 151.